ACS OMEGA

Open Access

http://pubs.acs.org/journal/acsodf

Article

Pure Component and Binary Mixture Adsorption of Light Alkanes and Alkenes on Zeolite NaX at Low Temperatures: Influence of Chain Length

Mats Roehnert, Christoph Pasel,* Christian Bläker, and Dieter Bathen

Cite This: *ACS Omega* 2024, 9, 37548−37559

Read Online

ACCESS | Metrics & More | Article Recommendations | Supporting Information

ABSTRACT: In this study, the separation of short-chain alkane/alkene pairs by fixed-bed adsorption on zeolite NaX at low temperatures is investigated. Experiments are carried out with pure components and mixtures of ethane/ethene, propane/propene, and *n*-butane/1-butene in the temperature range between −75 and +40 °C and partial pressures up to 450 Pa. For a short chain length, much stronger adsorption of the alkene is observed. In contrast, with an increase in chain length, the isotherms of alkanes and alkenes of the same chain length become more similar. In addition, a greater influence of temperature on capacity is seen, the shorter the chain length is. In binary mixtures, a strong competition occurs at high total loadings with the alkene displacing the alkane. A characteristic curve is formed for the selectivity in the mixture, which shifts to higher temperatures with an increase in the chain length.

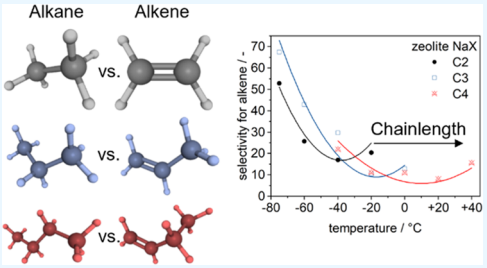

1. INTRODUCTION

Separation of alkanes and alkenes of the same chain length is a sophisticated task in the chemical industry, since they often have similar physicochemical properties. Moreover, the difference between these properties decreases with increasing chain length. While the difference between the boiling points of ethane and ethene is 15.1 K, it is only 5.8 K for *n*-butane and 1-butene. One option for separating these substances is adsorption, which is already used for separating butane isomers. Adsorptive separation is based on different temperature-dependent interactions with a solid surface. Since zeolites in particular are industrially relevant and, due to their uniform crystal structure, are well suited for systematic investigation, they are used in this work. In the literature, there are already some studies dealing with the adsorption of hydrocarbons on zeolites.

Chung et al.[1] investigated pure component kinetics and thermodynamics of the C2 hydrocarbons ethane and ethene on a 13X zeolite at temperatures from 30 to 70 °C. Adsorption isotherms were recorded up to a pressure of 600 kPa. The authors found higher adsorption enthalpies and a more pronounced increase in isotherms in the low partial pressure range for adsorption of ethene, which they attributed to strong cation-π interactions between sodium cations of the zeolite and the π-bonding of ethene. For ethane, in contrast to ethene, the isosteric enthalpy of adsorption increases with increasing loading due to lateral interactions. The comparison with the C3 hydrocarbons propane and propene shows that the difference in adsorption affinity between alkane and alkene becomes smaller with increasing chain length.

Through Monte Carlo simulations, Henson et al.[2] identified different adsorption mechanisms for ethane and ethene on a NaY zeolite. While the zeolite represents a homogeneous surface for ethane with many energetically similar adsorption sites, there are two adsorption sites for ethene of different energetic value.

Danner and Choi[3] investigated pure component and multicomponent adsorption of ethane and ethene at 25 and 50 °C on a 13X zeolite. The experimental results show a preference of zeolite for ethene and a low-temperature dependence of the selectivity in the mixture. In contrast, Mofarahi and Salehi[4] used the vacancy solution theory to show that the selectivity of a 5A zeolite for ethene increases with lowering of the temperature.

An increase in selectivity for the alkene with lower temperature was also shown by van Miltenburg et al.[5] They measured pure component and mixture isotherms of propane and propene on faujasite zeolites at temperatures between 45 and 135 °C and observed higher selectivities for lower temperatures. A higher affinity of the zeolite for the alkene compared with the alkane was also seen for the C3 hydrocarbons.

Jarvelin and Fair[6] investigated the adsorptive separation of propane and propene on different zeolites and found that a 13X

Received: December 13, 2023
Revised: July 14, 2024
Accepted: August 6, 2024
Published: August 25, 2024

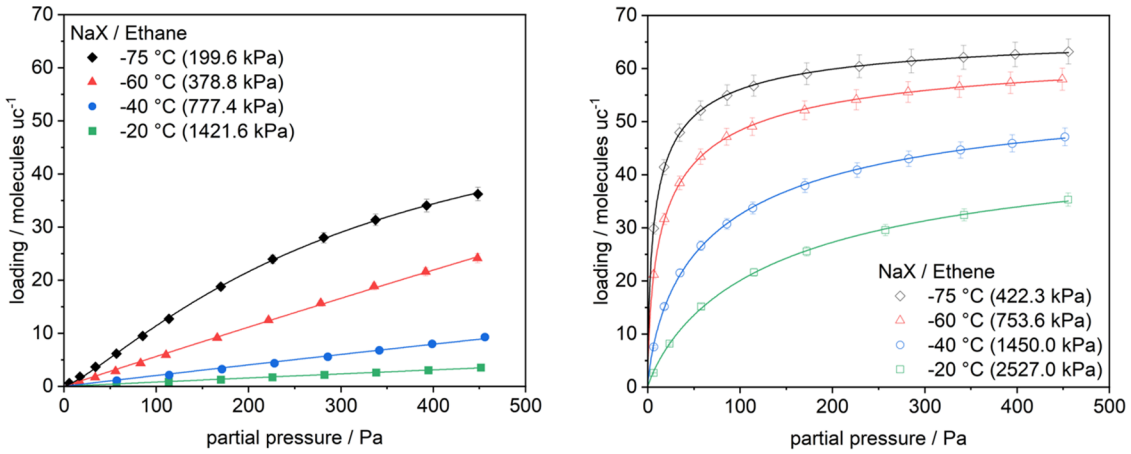

Figure 1. Adsorption isotherms of ethane (left) and ethene (right) on zeolite NaX at temperatures −20 °C (green squares), −40 °C (blue circles), −60 °C (red triangles), and −75 °C (black diamonds). The saturation pressure is given in parentheses after each temperature.

zeolite had the highest capacity. In addition, kinetic experiments showed a roll-up effect for propane, which is attributed to displacement by propene.

A pronounced displacement of the alkane by the alkene was also observed by Campo et al.[7] in the adsorption of propane and propene on a 13X zeolite. The concentration of propane in a binary breakthrough curve at 100 °C was more than 3 times higher than the input concentration as a result of the roll-up, which demonstrates the strong displacement of the alkane by the alkene.

Huang et al.[8] determined pure component and mixture isotherms of propane and propene on a zeolite 13X at 25, 50, and 70 °C. The mixture experiments were conducted at constant total concentration and varying gas phase composition. The authors found that the two hydrocarbons competed strongly for available adsorption sites with the alkene exhibiting the higher affinity. It was also found that the selectivity decreased with increasing temperature for the same gas phase composition.

There are only a few data available for a mixture of the C4 hydrocarbons *n*-butane and 1-butene. For example, Wang et al.[9] studied the separation of ZSM5 zeolites with different Si/Al ratios. The higher the Al content of the zeolites, the higher capacities were achieved for 1-butene. The prediction of the ideal adsorbed solution theory showed the highest selectivity for the zeolites with a high Al content.

Thamm et al.[10] investigated calorimetrically the pure component adsorption of *n*-butane and 1-butene on different adsorbents. The authors explain the higher adsorption enthalpy of 1-butene at low loadings with cation-π bonds between the cations of the zeolite and π-electrons of the alkene.

Further work investigating the adsorption properties of C4 hydrocarbons either deals with pure component measurements, isomer mixtures, or focuses on the use of different adsorbents.[11−14]

The influence of chain length on pure component adsorption of alkanes was investigated by Birkmann et al.[15] The authors determined isotherms of ethane, propane, and *n*-butane between −40 and +60 °C on an activated carbon and a zeolite 13X. They found an increase in adsorption capacity with increasing chain length due to the higher number of binding sites as well as higher polarizability. Lowering the temperature had the same effect, with the greatest influence on the shortest-chain alkane ethane.

In summary, many of the papers presented investigate only one alkane/alkene pair or focus on the properties of adsorbents. A systematic study in which the chain length of alkane/alkene pairs is varied, and thus the influence of the chain length on the adsorption properties at different temperatures is investigated in detail, is not yet available.

The aim of this work is to investigate the influence of chain length and temperature on the adsorption of C2 to C4 alkanes and alkenes in pure component adsorption and in mixture adsorption on a zeolite NaX, which was found to be well suited for the separation of ethane and ethene in a previous work.[16] Particular attention will be paid to the competitive effects that occur between the adsorptives. In addition, a recommendation for technical applications will be given on the basis of selectivity parameters.

2. RESULTS AND DISCUSSION

Pure component isotherms (Figures 1−5) and mixture isotherms (Figures 6−8) of the hydrocarbons ethane, ethene, propane, propene, *n*-butane, and 1-butene were measured on a zeolite NaX at temperatures between −75 and +40 °C. The results of the pure component experiments are presented in the form of isotherm fields. The loadings are plotted in molecules per unit cell against the partial pressure in Pa. The mixture diagrams show the experimental data of the pure component experiments and the mixture measurements, with the partial pressure of the alkane plotted on the lower *x*-axis and the partial pressure of the alkene plotted on the upper *x*-axis. The symbols show the measured data. The solid lines represent the fit of the pure component isotherms to the Sips isotherm. All fits achieve a coefficient of determination of $R^2 > 0.99$. The Sips parameters are in valid ranges for the measurement data and are given in the Supporting Information (SI). For the sake of brevity, only the results of the highest and lowest temperatures are shown for the mixture experiments. All data and also the diagrams for the temperatures in between can be found in the SI. At this point, it should be mentioned that the C2 hydrocarbons data have already been published in a previous paper.[16]

2.1. Pure Component Adsorption. Figure 1 shows the pure component isotherms of the C2 hydrocarbons ethane (left) and ethene (right) on zeolite NaX at temperatures −20, −40, −60, and −75 °C. The adsorption isotherms of ethane are mostly linear. This indicates an energetically homogeneous surface for ethane with constant, weak interactions. Only the isotherm at −75 °C is slightly right-curved. On the one hand, this can result from a saturation of adsorption sites and, on the

https://doi.org/10.1021/acsomega.3c09951
ACS Omega 2024, 9, 37548−37559

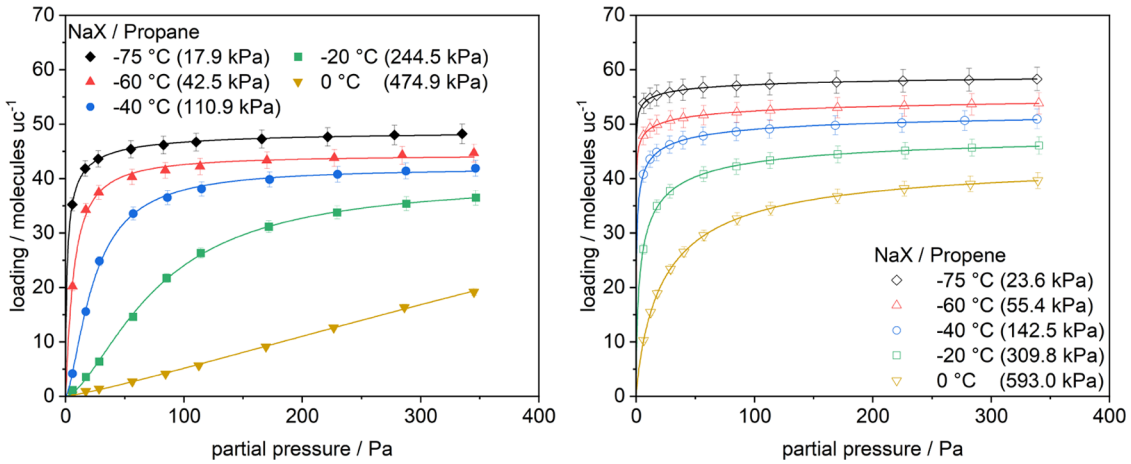

Figure 2. Adsorption isotherms of propane (left) and propene (right) on zeolite NaX at temperatures 0 °C (yellow triangles), −20 °C (green squares), −40 °C (blue circles), −60 °C (red triangles), and −75 °C (black diamonds). The saturation pressure is given in parentheses after each temperature.

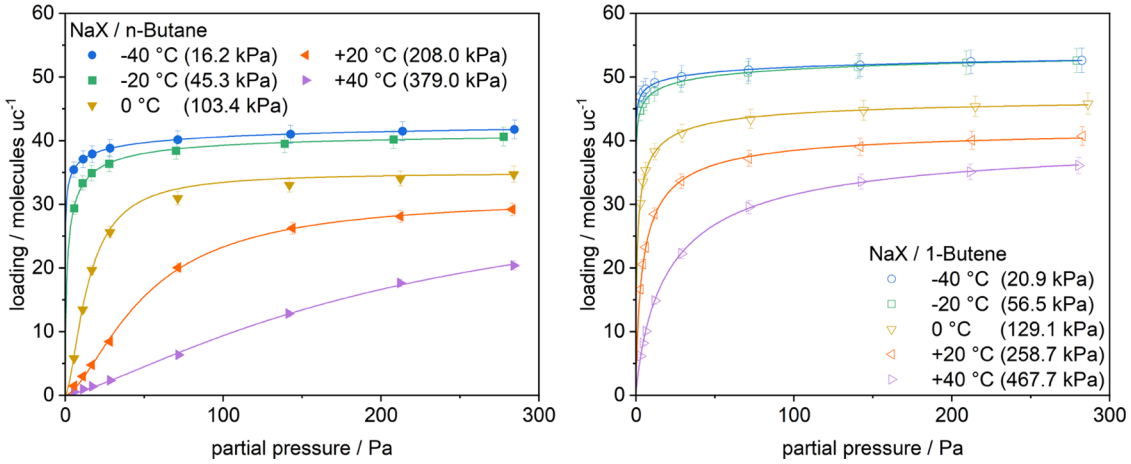

Figure 3. Adsorption isotherms of *n*-butane (left) and 1-butene (right) on zeolite NaX at temperatures +40 °C (purple triangles), +20 °C (orange triangles), 0 °C (yellow triangles), −20 °C (green squares), and −40 °C (blue circles). The saturation pressure is given in parentheses after each temperature.

other hand, be caused by an energetic heterogeneity of the adsorbent surface. The curvature starts when a loading of about 24 molecules per unit cell is reached. This corresponds to the number of cations at position III/III′. The ethane molecules apparently occupy the cations at this position primarily. As soon as all cations of position III/III′ are saturated, the molecules attach to another adsorption site, presumably to cations on position II. These seem to be of lower energetic value, resulting in the described curvature of the isotherm. The adsorption isotherms of ethene are consistently curved to the right and, except for the isotherm at −75 °C, do not reach saturation. This indicates a heterogeneous surface and thus energetically different adsorption sites for the alkene. Lowering of the temperature leads to a stronger curvature of the isotherms. Energetically less favorable adsorption sites at low temperatures are therefore already occupied at lower partial pressures. At −75 °C, the loading increases only slightly above a partial pressure of about 150 Pa. The isotherm transitions to a saturation plateau, which is about 65 molecules per unit cell. Bläker et al.[17] report a similar value of the saturation loading of ethene on a NaX zeolite. Since the number of accessible cations is about 56 cations per unit cell, the additional ethene molecules appear to either form lateral interactions or attach to the zeolite framework. Another possibility would be that more than one molecule would attach to more than one cation. When the two hydrocarbons are compared, it can be seen that ethene adsorbs much more strongly than ethane at all temperatures. This can be attributed to the cation-π interactions between the π-electrons of ethene and the sodium cations of the zeolite.

The adsorption isotherms of propane on zeolite NaX shown in Figure 2 are mostly right-curved. Only the isotherm at 0 °C is linear. As for ethane, the isotherms are linear up to a loading of approximately 24 molecules per unit cell while the molecules adsorb to cations at position III, until a change of the cation position occurs. For temperatures below −40 °C, the isotherms enter a saturation plateau, which shifts to higher loading values as the temperature is lowered. The increase in saturation loading can be explained by assuming that the adsorbed phase is in a liquid-like state in the range of pore saturation. The density of a liquid increases with lowering of the temperature. This effect is also observed in the saturation plateaus of propane isotherms as more molecules fit into the unit cell. The propene isotherms approach saturation at all temperatures, with loadings higher than those of propane. This can be explained by the size of the molecule. Because of the double bond, propene has two hydrogen atoms less than propane, and the double bond leads to

https://doi.org/10.1021/acsomega.3c09951
ACS Omega 2024, 9, 37548−37559

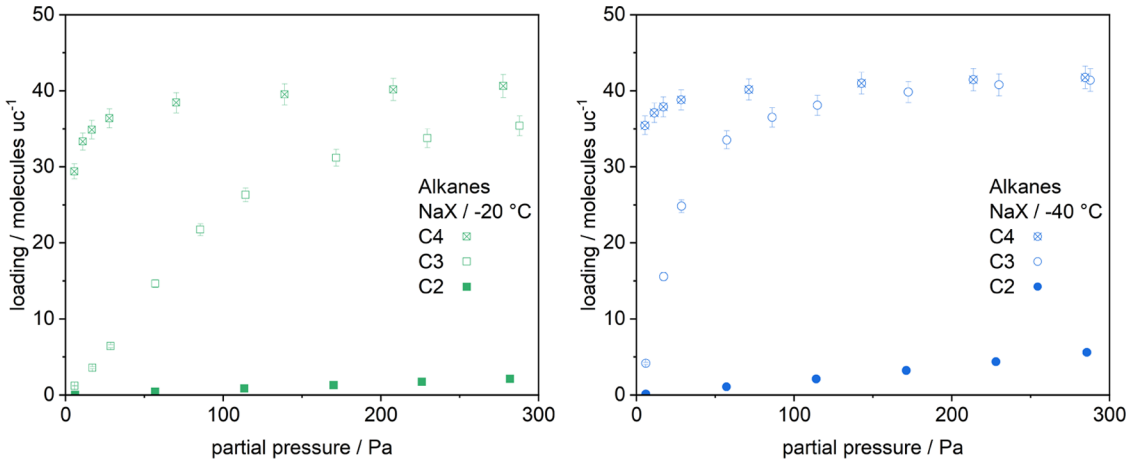

Figure 4. Adsorption isotherms of ethane (filled symbols), propane (empty symbols), and *n*-butane (crossed-out symbols) on zeolite NaX at temperatures −20 °C (left) and −40 °C (right).

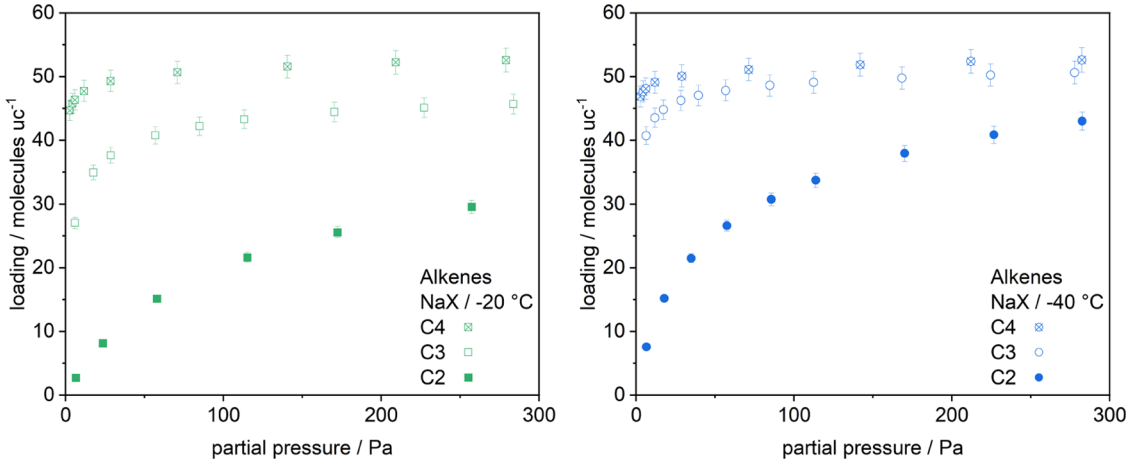

Figure 5. Adsorption isotherms of ethene (filled symbols), propene (empty symbols), and 1-butene (crossed-out symbols) on zeolite NaX at temperatures −20 °C (left) and −40 °C (right).

a smaller bond length between the carbon atoms, so the molecular volume of propene is smaller. When the C3 hydrocarbons are compared, it is noticeable that the difference between the isotherms at the same temperature is smaller than between ethane and ethene. This can be attributed to the greater structural similarity of the C3 hydrocarbons, which both have a single bond and differ only in the second bond, which is a single bond in the alkane and a double bond in the alkene. In the case of C2 hydrocarbons, the alkane has a single bond, and the alkene has a double bond.

The adsorption isotherms of *n*-butane on zeolite NaX are given in Figure 3. A curvature of the isotherm already occurs at +40 °C and increases with lower temperature. In contrast to the isotherms of ethane and propane, the isotherms of *n*-butane already show a curvature below a loading of 24 molecules per unit cell. Thus, the interactions do not occur exclusively with the cations at position III. Presumably, the *n*-butane molecules, with a length of 7.86 Å, are so large that they can interact with several cations simultaneously, and the zeolite thus does not offer an energetically homogeneous surface for *n*-butane. According to Mellot-Draznieks et al.,[18] the distances between the cations are between 4.7 and 6.2 Å. The identical saturation plateaus at temperatures of −20 and −40 °C are also remarkable. Unlike the other hydrocarbons, a decrease in the temperature in this range no longer leads to an increase in saturation loading. Only the slope in the initial partial pressure range increases. The constant capacity is probably due to steric hindrance during adsorption. Due to their size and positioning, the molecules block access to the adsorption sites for other adsorptive molecules. The same effect also occurs in the adsorption isotherms of 1-butene. Again, the isotherms reach the same saturation loading at −20 and −40 °C. As in the case of C_3 hydrocarbons, this is somewhat higher for the alkene than for the alkane due to the smaller molecular volume.

Figure 4 compares the adsorption isotherms of the C2, C3, and C4 alkanes ethane, propane, and *n*-butane at −20 °C (left) and at −40 °C (right). At both temperatures, the isotherms arrange according to chain length. In addition, a longer chain length leads to a stronger curvature of the adsorption isotherm and thus to saturation starting at lower partial pressures. This can be attributed to the dispersion and induction interactions that the alkanes form with the zeolite. Crucial for this type of interaction are the number of binding sites and the polarizability. Both properties increase with increasing chain length, which leads to a stronger interaction and higher loadings. The loading difference between the adsorption isotherms decreases with greater chain length. On average, the zeolite has a 25 times higher capacity for propane than for ethane. The capacity for *n*-

https://doi.org/10.1021/acsomega.3c09951
ACS Omega 2024, 9, 37548−37559

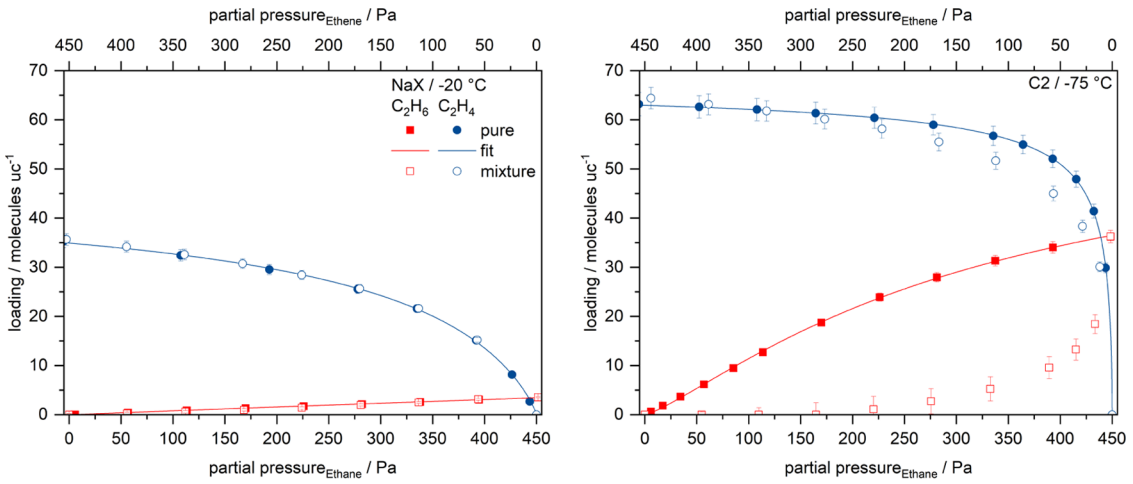

Figure 6. Pure component (filled symbols) and mixture (empty symbols) adsorption isotherms of the C2 hydrocarbons ethane (red) and ethene (blue) on zeolite NaX at −20 °C (left) and −75 °C (right) and a constant total adsorptive pressure of 450 Pa. Continuous lines: pure component fit with the Sips equation.

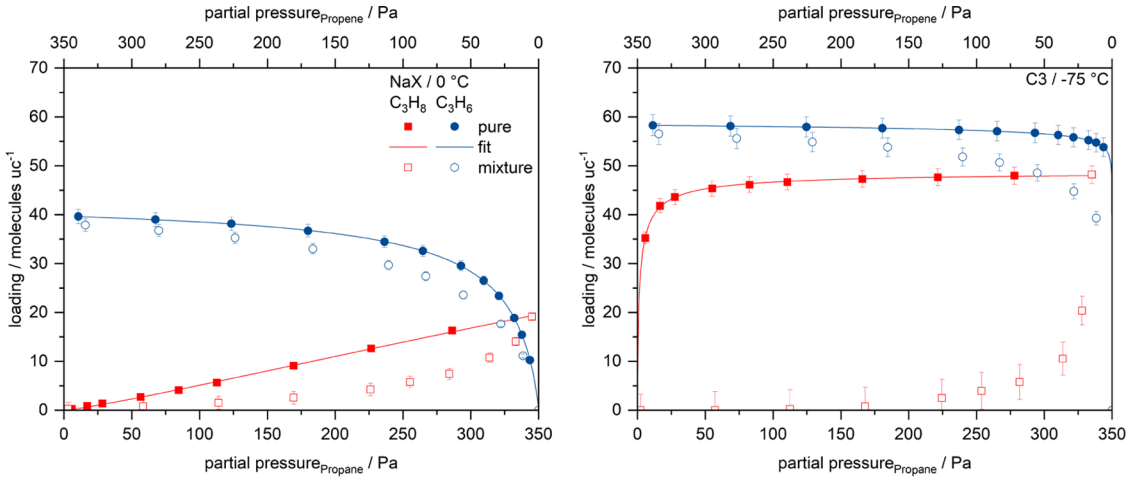

Figure 7. Pure component (filled symbols) and mixture adsorption (empty symbols) isotherms of the C3 hydrocarbons propane (red) and propene (blue) on zeolite NaX at 0 °C (left) and −75 °C (right) and a constant total adsorptive pressure of 350 Pa. Continuous lines: pure component fit with Sips equation.

butane, on the other hand, is on average only 10 times as high as that for propane. The differences also become smaller with lower temperatures. At −40 °C, the propane capacity is only 17 times as high as the ethane capacity, and the capacity of *n*-butane is on average only 3 times that of propane. It can be concluded that increasing chain length leads to smaller differences in adsorption properties. This can be explained by the percentage change in the molecular structure. While the chain length difference of ethane to propane is one carbon atom, i.e., 50% of the chain length of ethane, the chain length of propane to *n*-butane increases by only 33%. The temperature influence on the small chain lengths is greater, which is mainly due to the fact that the longer-chain molecules already approach saturation at higher temperatures and can therefore no longer benefit as much from a temperature reduction.

The isotherms of the alkenes ethene, propene, and 1-butene at −20 °C (left) and −40 °C (right) in Figure 5 reveal that a longer chain leads to earlier saturation, as has been observed for the alkanes. However, the difference between the chain lengths is less pronounced for alkenes than for alkanes. At −20 °C, the propane capacity is about 3 times the capacity of ethene, while the capacity of 1-butene is only by a factor of 1.2 higher than the capacity of propene. Lowering the temperature to −40 °C results in the propane capacity being 1.8 times higher than the ethene capacity and the 1-butene loading is on average only 1.06 times higher than that of propene. The smaller difference between the adsorption isotherms can be attributed to the fact that cation-π interactions dominate the adsorption of alkenes. Since all three molecules have a π-bond and can thus form this type of interaction, the difference in adsorption properties is consequently smaller. In addition, as for alkanes, it can be seen that the temperature effect is greatest on the shortest-chain molecule, since the isotherms of the longer-chain molecules are already approaching saturation.

Plotting the loadings against the relative pressures provides a different insight when comparing molecules of different chain lengths. Figure S13 in the SI shows the loadings on zeolite NaX at −20 and −40 °C as a function of the relative pressure. The curves of the isotherms in these diagrams support the theory that the adsorption properties of the hydrocarbons become more similar to increasing chain length. For example, the isotherms of propene and 1-butene at −40 °C are almost identical in the

https://doi.org/10.1021/acsomega.3c09951
ACS Omega 2024, 9, 37548−37559

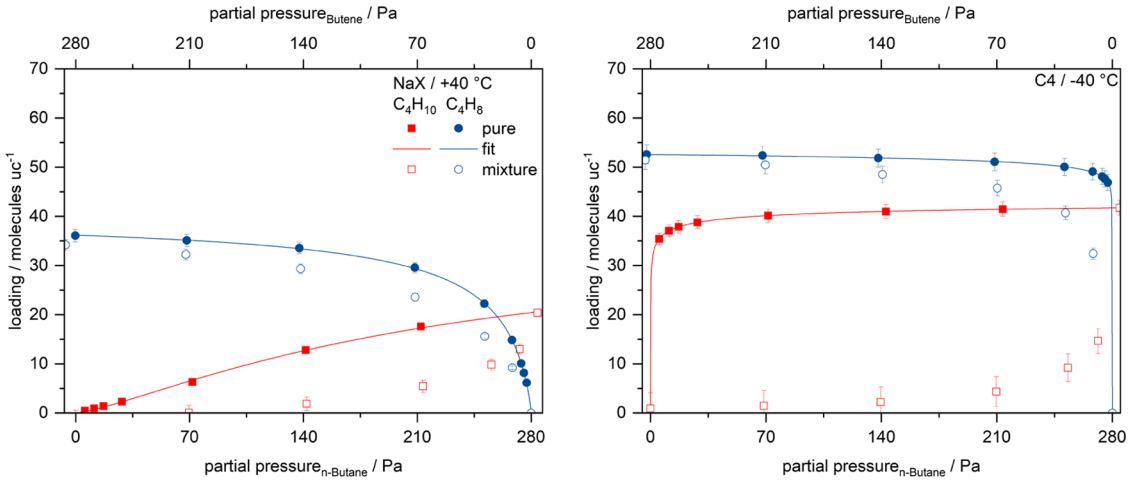

Figure 8. Pure component (filled symbols) and mixture adsorption (empty symbols) isotherms of the C4 hydrocarbons *n*-butane (red) and 1-butene (blue) on zeolite NaX at +40 °C (left) and −40 °C (right) and a constant total adsorptive pressure of 280 Pa. Continuous lines: pure component fit with Sips equation.

relative pressure range investigated. Only in the initial range at low relative pressures, the isotherm of the C4 alkene is at slightly higher loadings. For reasons of brevity, however, this form of presentation is not used more extensively.

2.2. Binary Mixture Adsorption. Figure 6 shows the pure component and mixture isotherms of ethane and ethene on zeolite NaX at temperatures of −20 °C (left) and −75 °C (right). At −20 °C, there is no visible difference between the pure component and mixture isotherms. Taking into account the error bars are taken into account, the difference between the pure component loading and the mixture loading of ethane at an equimolar gas phase composition ($p_{ethane} = p_{ethene}$ = 225 Pa), as an example, is only 4%. Thus, there is only a small displacement of ethane by ethene and there seems to be sufficient adsorption sites for both adsorptives. Assuming that 56 cations are available as adsorption sites in a unit cell, and with a total loading of maximum 35 molecules per unit cell, the slight displacement is plausible. When the temperature is lowered to −40 °C, the displacement increases to 46% with equimolar gas phase composition. Ethene forms stronger interactions than ethane due to the double bond and displaces the alkane from energetically valuable adsorption sites. With further temperature reduction, the displacement of ethane by ethene increases. There is a pronounced competitive situation since there are no longer sufficient adsorption sites available for both adsorptives. At −75 °C, ethane is almost completely displaced at an equimolar gas phase composition. However, it is also apparent that at low levels of ethene in the gas phase, even the alkene does not reach the pure component loading. Accordingly, ethane seems to block some of the energetically valuable adsorption sites where ethene would adsorb. Only with decreasing ethane fraction, these sites are occupied by ethene.

Figure 7 shows pure component and mixture isotherms of the C3 hydrocarbons at 0 (left) and −75 °C (right). At 0 °C, a marked displacement of propane by propene can be seen, which amounts to 72% in the equimolar gas phase. Unlike in the ethane/ethene mixture, saturation of the adsorption sites and thus competition for these sites already begins at 0 °C due to the greater chain length. The degree of displacement increases further with decreasing temperature. At −75 °C, almost complete displacement is already achieved at equal partial pressures. For lower temperatures, the propene loading in the mixture continues to increase slightly, while the pronounced displacement is already evident at lower propene partial pressures.

The pure component isotherms of the two hydrocarbons show very similar curves at −75 °C with a steep increase at low partial pressures and saturation loadings, which differ by only about 10%. Nevertheless, strong displacement of the alkane occurs. This can be explained on the basis of the enthalpy differences between the alkane and alkene and the probability with which a molecule occupies an adsorption site. The ratio of the probabilities that a molecule is in a state 1 or a state 2 can be expressed using the Boltzmann factor and depends on the energies E_1 and E_2 in states 1 and 2 and the absolute temperature T.

$$\frac{P(E_2)}{P(E_1)} \propto \frac{\exp\left(-\frac{E_2}{RT}\right)}{\exp\left(-\frac{E_1}{RT}\right)} = \exp\left(\frac{-\Delta E_{21}}{RT}\right) \tag{1}$$

In the case of adsorption, this expression is useful because it is the ratio of probabilities for a molecule to be in the fluid phase (state 1) or to be adsorbed on the surface (state 2), where $\Delta E_{21} = \Delta h_{ads}$ which is the heat of adsorption. So, it describes the probability of occupying an adsorption site. Then, to assess the competition in the mixture adsorption of alkane and alkene, the ratio of site occupation probabilities is calculated by eq 2

$$\frac{\left(\frac{P(E_2)}{P(E_1)}\right)_{alkane}}{\left(\frac{P(E_2)}{P(E_1)}\right)_{alkene}} \propto \frac{\exp\left(\frac{-\Delta h_{ads,alkane}}{RT}\right)}{\exp\left(\frac{-\Delta h_{ads,alkene}}{RT}\right)} = \exp\left(\frac{-(\Delta h_{ads,alkane} - \Delta h_{ads,alkene})}{RT}\right) \tag{2}$$

According to Bläker et al.,[19] the differences between the heats of adsorption of alkane and alkene on zeolite NaX are about 5 kJ·mol^{-1} for the C2 hydrocarbons and 10 kJ·mol^{-1} for the C3 and C4 hydrocarbons. A calculation of the adsorption enthalpies for the data measured in this publication was carried out using the isosteric method for the C2 molecules ethane and ethene. While ethane has an average isosteric adsorption enthalpy of approximately 19.73 kJ·mol^{-1} in the loading range investigated,

https://doi.org/10.1021/acsomega.3c09951
ACS Omega 2024, 9, 37548−37559

the adsorption enthalpy of ethene averages 29.77 kJ·mol^{-1}. Accordingly, the difference in the adsorption enthalpies is in a similar range to the values determined by Bläker et al. Applying the isosteric method to the isotherm fields of longer-chain molecules is not a viable option due to the strongly curved isotherms and the resulting small loading ranges in which the isotherms overlap. The probability ratio alkane/alkene (left side of eq 10) depends exponentially on the difference in the heats of adsorption ($\Delta h_{ads,alkane} - \Delta h_{ads,alkene}$), which leads to a strong displacement of the alkane despite similar isotherms and saturation loadings. For example, at a temperature of 313.15 K, the ratio is 0.0215 for a difference of 10 kJ·mol^{-1}. Further exemplary values for other differences and temperatures can be found in the SI.

The mixture and pure component isotherms of *n*-butane and 1-butene from −40 to +40 °C are shown in Figure 8. As with the C3 hydrocarbons, displacement begins at high temperatures. Thus, at a partial pressure of 140 Pa and a temperature of +40 °C, the loading of *n*-butane in the mixture is already 85% lower than in pure component adsorption. The displacement increases further with lowering of the temperature and is highest at −40 °C with 95%. As in the case of the C3 hydrocarbons, strong displacement occurs despite similar isotherms, which can again be explained using the Boltzmann factor with the resulting exponential dependence of the difference of the heats of adsorption (eq 2).

The curves of the selectivities shown in Figure 9 illustrate the quotient of the alkene and alkane loading at equimolar gas phase

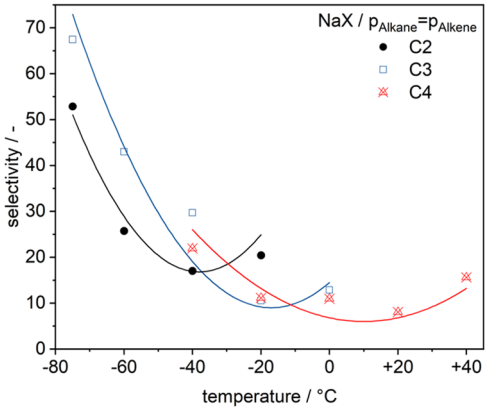

Figure 9. Selectivity of alkane/alkene separation in a binary mixture of C2 (filled circles, black), C3 (empty squares, blue), and C4 (crossed-out triangles, red) hydrocarbons for equimolar adsorptive composition of the gas phase dependent on the temperature.

composition as a function of the temperature. The selectivities exhibit similar curves for all three chain lengths. Coming from high temperatures, the selectivity decreases to a minimum and then increases again for lower temperatures. The decrease in selectivity with lowering of the temperature is due to the greater percentage increase in the loading of the alkane compared to that of the alkene. This is due to the increasing total loading in the mixture, which is mainly provided by the loading of the alkene. Thereby, the increasing loading supports the adsorption of the alkane by lateral dispersion interactions with the predominantly present alkene molecules. We were able to prove this observation in a previous work using the ideal adsorbed solution theory.[16] The increase with further temperature reduction occurs due to saturation effects. The total loadings are so high in this region that the adsorptives compete for every available adsorption site. Since in this competitive situation the alkene is preferentially adsorbed and the alkane is strongly displaced, the selectivity increases. Furthermore, a shift of the minima to higher temperatures can be observed with an increase in the chain length. With an increase in chain length, saturation is already reached at higher temperatures. Accordingly, strong competition and displacement also begin at higher temperatures.

Figure 10 shows the performance factors of the hydrocarbon separation as a function of temperature with equimolar gas phase

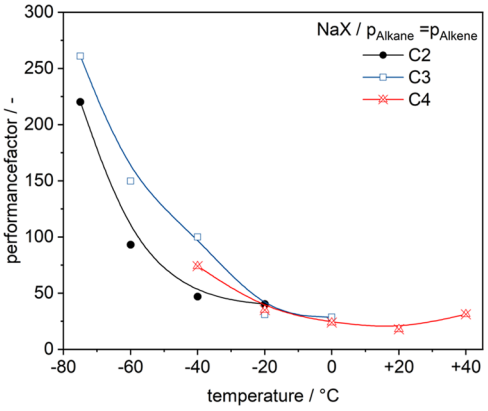

Figure 10. Performance of alkane/alkene separation in a binary mixture of C2 (filled circles, black), C3 (empty squares, blue), and C4 (crossed-out triangles, red) hydrocarbons for equimolar adsorptive composition of the gas phase dependent on the temperature.

composition in the mixture. The performance factor contains the loading difference between alkane and alkene. As in the case of small loadings the difference is also small, the performance factor becomes marginal in contrast to the selectivity. So, it is a more suitable number to asses technical applicability than selectivity. While the performance factor of the C4 hydrocarbons passes through a minimum, it increases continuously for the C2 and C3 hydrocarbons in the temperature range investigated as the temperature is lowered. In combination with the selectivity, a temperature below −40 °C is recommended for the separation of C2 hydrocarbons. For the separation of the C3 hydrocarbons, a positive effect is already visible at temperatures <−20 °C. For the C4 mixture, only a temperature reduction to −40 °C has a clear positive effect on the separation efficiency. Although the selectivity at this temperature is not much greater than at +40 °C, the loadings achieved are higher so that the performance factor reveals the favorable effect of temperature reduction in the case of the C4 mixture. For a technical application, however, not only the selectivities and the achievable capacities are important, but also other factors such as the working capacities in a cyclic process, the adsorption and desorption rates, and the desorption conditions. Both the calculated selectivities and the performance factors only serve as an initial indication of the operating conditions for a technical process.

3. SUMMARY AND CONCLUSIONS

In this study, pure component and multicomponent adsorption of the alkane/alkene pairs ethane/ethene, propene/propene, and *n*-butane/1-butene was investigated on zeolite NaX at temperatures between −75 and +40 °C. Special attention was

https://doi.org/10.1021/acsomega.3c09951
ACS Omega 2024, 9, 37548−37559

paid to the difference in adsorption properties between alkane and alkene at different temperatures and to the influence of the chain length.

During adsorption of the pure component, a significantly stronger adsorption of the alkene can be observed compared to that of the alkane. This is attributed to the additional π-bond of the alkenes, which forms interactions with the cations of the zeolite. With increasing chain length, the difference between the adsorption properties of the alkane and alkene becomes smaller because the molecule structure becomes more similar. Also, an increase in chain length within the groups of alkanes and alkenes causes the adsorption isotherms to become more similar. This effect becomes stronger as the temperature is lowered since the longer-chain hydrocarbons are already saturated and no longer benefit from the lower process temperature.

In the binary mixture of alkane/alkene pairs, pronounced displacement effects by competitive adsorption are observed in many cases. While competition for adsorption sites only occurs at low temperatures for C2 hydrocarbons, a longer chain length leads to displacement already occurring at higher temperatures. Despite similar pure component isotherms of the alkane and alkene, the C3 and C4 mixtures show a strong displacement. The competition for adsorption sites can be described using site occupation probabilities resulting from the Boltzmann distribution. The strong displacement is attributed to the exponential dependence of the distribution on the difference of the heats of adsorption of alkane and alkene.

The selectivity shows similar curves for the different chain lengths and is strongly dependent on the total loading of the zeolite. An increase in chain length leads to a shift of the selectivity curve to higher temperatures. The separation efficiency increases for all alkane/alkene pairs below a temperature of −20 °C.

In further work, the influence of the temperature on the adsorption of hydrocarbon isomer mixtures will be investigated. Since the measurements in this work were made at low partial pressures and, in the case of the C2 hydrocarbons, displacement effects were only observed at very low temperatures, experiments will be carried out at higher concentrations in order to investigate the influence of the concentration. In addition, it might be of interest to investigate further zeolitic adsorbents with other structures or cations. Furthermore, various models for predicting mixture adsorption based on pure component isotherm data can be applied and evaluated. A first test of the multi-Sips model for predicting the mixture adsorption of ethane and ethene at −75 °C provides promising results (see Figure S14 in the SI).

4. EXPERIMENTAL SECTION

4.1. Materials. The adsorbent used in this work is a binder-free faujasite zeolite (FAU) obtained from Chemiewerk Bad Köstritz GmbH. The idealized, crystalline lattice structure of this material is shown in Figure 11 and is composed of double six-membered rings (D6R) and sodalite cages. The large cavity that is formed in the center of this structure is called a supercage.

The investigated zeolite has a Si/Al ratio of 1.175 and can thus be assigned to type X zeolites. The composition of a unit cell (smallest repeating unit) of the investigated zeolite can be described by the expression in eq 3.

$$Na_{88}^{+}Al_{88}Si_{104}O_{384} \quad (3)$$

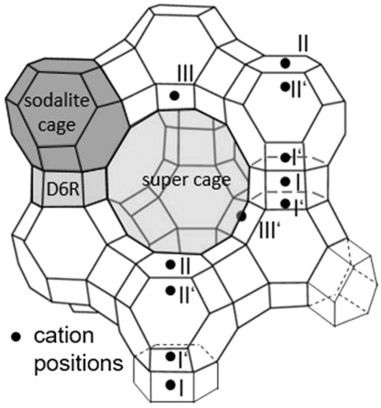

Figure 11. Framework topography of the FAU structure with framework cations I−III′. Adapted with permission from ref 20. Copyright 2021 by the authors, MDPI.

It can be seen that the material is a zeolite containing only single-charged sodium cations. In the following, the material is therefore referred to as NaX.

The sodium cations can be located at the positions indicated by the Roman numerals in Figure 11. For the adsorption of the investigated adsorptives, positions II, III, and III′ are most relevant, since positions I, I′, and II′ are located in the sodalite cages and double-six rings of the zeolite structure and are not accessible to the adsorptive molecules due to steric hindrance.[21,22] Position II is located in the supercage at the six-ring of the sodalite cage. Position III is located in the supercage at the four-ring surface of the sodalite cages, while position III′ is formed by a shift of the cations from position III toward the four-ring surfaces of the double-six rings.[23−25] The distribution of the 88 sodium cations present in the investigated zeolite is carried out according to the distribution proposal of Kulprathipanja.[21] Accordingly, 32 cations are located at position I′, which is not accessible to adsorptives. Another 32 cations are located at position II in the supercage, and the remaining 24 cations are located at position III/III′. However, this distribution is idealized and may show variations in reality due to different synthesis, activation, or conditioning methods. However, the publication of Mauer et al.[20] shows a similar distribution of cations, as that of Kulprathipanja, in the adsorption of methane on a NaX zeolite. In addition, considerations regarding the reduction of repulsive interactions between cations and the tendency of cations to occupy positions as close as possible to the zeolite lattice support the proposed distribution. For adsorption, cations far away from the lattice, such as cations at positions III and III′, represent good adsorption sites. On these sites, the cations are well accessible to the adsorptives and allow a spatially favorable approach for the formation of strong interactions.[22] The zeolite was prepared according to a common synthesis route in the liquid phase.[21,22]

Volumetric nitrogen isotherms at 77 K were recorded using an Autosorb iQ instrument by Quantachrome Instruments to structurally characterize the zeolite. Prior to measurement, the adsorbent was conditioned for 6 h at 300 °C under a vacuum. The specific surface area of the zeolite was determined according to DIN ISO 9277 and has a value of 772.87 $m^2 \cdot g^{-1}$. In addition, the total pore volume according to Gurvich (DIN 66134) and the micropore volume according to Dubinin−Radushkevich (DIN 66135−3) were determined. These are almost identical

https://doi.org/10.1021/acsomega.3c09951
ACS Omega 2024, 9, 37548−37559

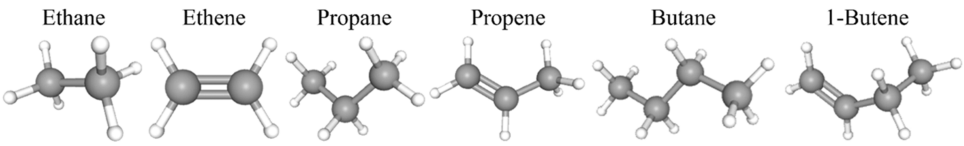

Figure 12. Molecular structure of the adsorptives[29] (carbon is gray, hydrogen is light gray).

Table 1. Chemical Sample Table of the Adsorptives[27,28,30−34]

	ethane	ethene	propane	propene	*n*-butane	1-butene
molecular formula	C_2H_6	C_2H_4	C_3H_8	C_3H_6	C_4H_{10}	C_4H_8
CAS Registry Number	74−84−0	74−85−1	74−98−6	115−07−1	106−97−8	106−98−9
supplier	air liquide	air liquide	air liquide	air liquide	air liquide	air liquide
purity/vol %	≥99.5	≥99.9	≥99.5	≥99.5	≥99.5	≥99.4
molar mass/g·mol^{-1}	30.07	28.05	44.10	42.08	58.12	56.11
1. dimension/Å	3.81	3.28	4.02	4.01	4.01	4.00
2. dimension/Å	4.08	4.18	4.52	5.08	4.52	5.10
3. dimension/Å	4.82	4.84	6.61	6.26	7.86	7.82
polarizability/10^{-30} m^3	4.47	4.25	6.29	6.26	8.20	7.97
dipole moment/10^{-30} C·m	0.00	0.00	0.28	1.22	0.17	1.00
quadrupole moment/10^{-40} C·m^2	3.34	6.67	4.01	8.34		

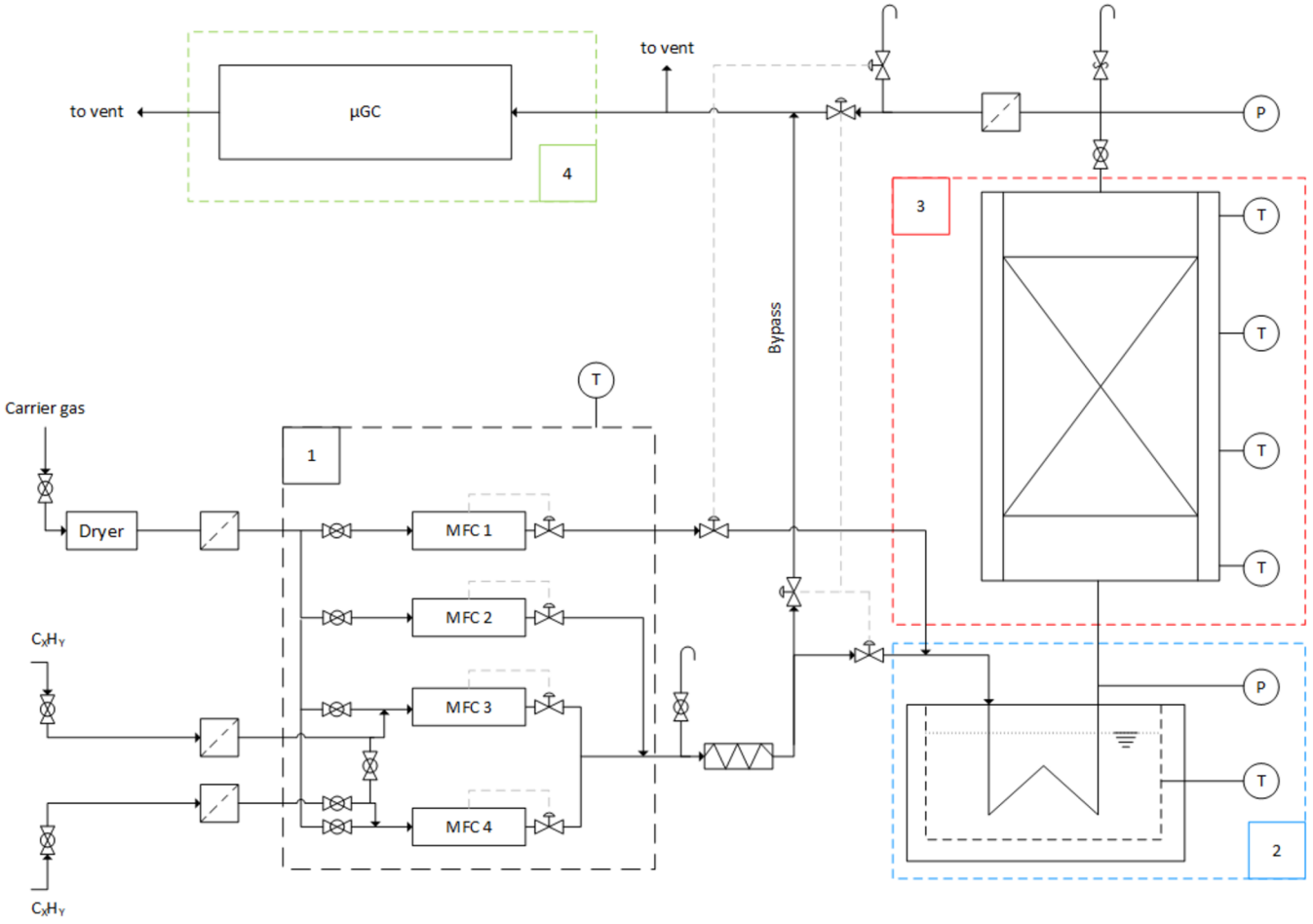

Figure 13. Flow sheet of the experimental setup: (1) gas-mixing chamber; (2) cooling thermostat; (3) fixed-bed adsorber; (4) micro gas chromatograph.[16]

with values of 0.321 cm^3·g^{-1} for the total pore volume and 0.316 cm^3·g^{-1} for the micropore volume.

The adsorptives used were the short-chain alkanes and alkenes ethane, ethene, propane, propene, *n*-butane, and 1-butene supplied by Air Liquide. Their molecular structures are shown in Figure 12. Relevant properties of the adsorptives are listed in Table 1. The molecular dimensions of propene and 1-butene were calculated with the software *ChemBio3D* using the MM2 energy minimization function,[26] while the dimensions of the other adsorptives are from the publications of Reid and

https://doi.org/10.1021/acsomega.3c09951
ACS Omega 2024, 9, 37548−37559

Thomas[27] and Webster et al.[28] The nitrogen used as carrier gas was supplied by the university's infrastructure and has a purity of >99.999%.

During the adsorption of short-chain hydrocarbons, various interactions between adsorptives and the adsorbent can occur. For example, a statistical charge shift in nonpolar molecules can lead to temporary polarization and thus to a mutual attraction of the dipoles formed. Cations of the zeolite and negative charges of the zeolite lattice can induce a dipole in polarizable molecules and, thus, form an interaction. In addition, interactions can occur between the quadrupole moments of alkenes and sodium cations or negative charges of the lattice.

In the interactions with the cations, the zeolite lattice also contributes to the interaction strength.[20] In the following, however, we will refer to the cations as the adsorption site since their contribution is greater.

Since the experiments take place in a nitrogen carrier gas stream, experiments termed pure component adsorption are in fact binary mixtures in which coadsorption effects with nitrogen may occur. These were quantified and found to be small in a previous study that investigated helium and nitrogen as carrier gases in the adsorption of short-chain hydrocarbons.[35] The authors found that the influence of the carrier gas decreases with increasing the chain length. While methane and nitrogen compete strongly for the available adsorption sites, the effect of changing the carrier gas from helium to nitrogen is already much lower for ethane. So, we assume that the impact is negligible for ethene and even more so for C3 and C4 hydrocarbons. Consequently, the adsorption of a mixture of alkane, alkene, and nitrogen is considered as a binary adsorption of two hydrocarbons.

4.2. Experimental Setup and Procedure. The experimental investigations were carried out on the laboratory plant shown in Figure 13. The hydrocarbons and the carrier gas nitrogen are dosed using thermal mass flow controllers, which are incorporated into a temperature-controlled box. The volume flow rates of the adsorptives can be varied between 1.84 and 90 mL·min^{-1}. Since the nitrogen flow is kept constant at 10 L·min^{-1}, the concentration is adjusted by varying the adsorptive flows. Due to different heat capacities, the maximum volume flows that can be dosed with the mass flow controllers also differ. As a result, the C4 hydrocarbons are measured up to a partial pressure of 280 Pa, while the C3 hydrocarbons are measured up to 350 Pa and the C2 hydrocarbons are measured up to a partial pressure of 450 Pa. This instrumental limitation does not affect the comparability of the results, since for the longer-chain molecules the loading range of the isotherms was recorded up to saturation, so the effect of displacement in binary adsorption is evident.

A thermostat operated with either ethanol or water, depending on the temperature of the experiment, is used to control the temperature of the experimental unit. The experimental setup allows for experiments at temperatures as low as −75 °C. A cooling coil is embedded in the thermostat bath, through which the gas flow is directed. In addition, part of the coolant is pumped through the double-jacketed adsorber in order to reduce the axial temperature gradient in the adsorber bed. For temperature monitoring, type T thermocouples are used, which are installed equidistantly in the adsorber. Pressure measurement upstream and downstream of the adsorber is carried out with pressure sensors from BD Sensors GmbH. The gas is streaming from bottom to top through the fixed-bed adsorber after temperature regulation. With a height of 20 cm and a diameter of 4 cm, the adsorber complies with the common design rules (height-to-diameter ratio between 3:1 and 5:1). Wall effects can also be neglected, since the ratio of particle diameter (2 mm) to adsorber diameter with a value of 20 is greater than 10.[36] The effluent gas stream is analyzed with a micro gas chromatograph (μGC, model Fusion) from INFICON with thermal conductivity detectors.

To ensure identical initial conditions before each experiment, the adsorbent is pretreated at 300 °C for 4 h in a nitrogen-purged oven. After pretreatment, the residual water content in the zeolite, determined by Karl Fischer titration, is 1.71 m.-%. The hot adsorbent is filled into the adsorber and then cooled to the desired experiment temperature with dry nitrogen. Before the experiment was started, the adsorptive concentration is adjusted by passing the gas flow over the bypass. As soon as the concentration is constant via the bypass, the adsorber can be charged with the gas flow, thus, starting the adsorption experiment.

If the concentration at the outlet of the adsorber is constant over a period of 30 min and has a relative standard deviation of less than 0.1%, the next equilibrium point of the isotherm can be set by increasing the adsorptive volume flow.

The binary mixture measurements were performed at a constant total adsorptive concentration. For this purpose, an alkane isotherm is measured up to the highest concentration. This is followed by a stepwise reduction of the alkane concentration, while the alkene concentration is increased by the same step size until only the alkene is present in the gas phase. Thus, only the gas phase composition is varied. An exemplary concentration profile for such a binary mixture measurement can be found in the SI.

4.3. Experimental Evaluation. The equilibrium loading of adsorbent X_{eq_i} can be determined by a mass balance around the adsorber. For this purpose, the area between the equilibrium concentration and the outlet concentration is calculated by integration. The indices i and j stand for the equilibrium point, and the measuring points for determining the equilibrium point. The molar flow $\dot{n}_{\mathrm{in}_i}$ is the total incoming molar flow, i.e., the sum of carrier gas and adsorptive, of the respective equilibrium point. The mass of the adsorbent is represented by m_{ads}. The quantity y_{in} represents the inlet concentration, which is calculated from the arithmetic mean of the outlet concentration y_{out} at equilibrium over a period of 20 min. The integration of the area is done by a summation of the concentration differences over time intervals Δt. Due to the cumulative design of the experiment, the loading of the previous points must be included.

$$X_{\mathrm{eq}_i} = X_{\mathrm{eq}_{i-1}} + \frac{\dot{n}_{\mathrm{in}_i}}{m_{\mathrm{ads}}} \cdot \sum_{j_{i,0}}^{j_{i,\mathrm{eq}}} \left(\frac{y_{\mathrm{in}_i} - y_{\mathrm{out}_j}}{1 - y_{\mathrm{out}_j}} \right) \cdot \Delta t_j \tag{4}$$

In the case of multicomponent adsorption, the concentration of the second component is taken into account. This results in the following equation for loading component 1

$$X_{\mathrm{eq}_{i,1}} = X_{\mathrm{eq}_{i-1,1}} + \frac{\dot{n}_{\mathrm{in}_i}}{m_{\mathrm{ads}}} \cdot \sum_{j_{i,0}}^{j_{i,\mathrm{eq}}} \left(y_{\mathrm{in}_{i,1}} - y_{\mathrm{out}_{j,1}} \cdot \left(\frac{1 - y_{\mathrm{in}_{i,1}} - y_{\mathrm{in}_{i,2}}}{1 - y_{\mathrm{out}_{j,1}} - y_{\mathrm{out}_{j,2}}} \right) \right) \cdot \Delta t_j \tag{5}$$

https://doi.org/10.1021/acsomega.3c09951
ACS Omega 2024, 9, 37548−37559

Due to the higher density of adsorptives in the adsorbed phase (liquid-like state) by an order of magnitude of 4−5 compared to the density in the gas phase, the mole numbers of adsorptives in the adsorbed phase are much larger than in the gas phase. Mole numbers of the adsorptives in the gas volume consisting of dead volumes in the piping and in the interstitial grain volume, which cause a dead time and thus a delayed concentration measurement, can therefore be neglected. A complete derivation of the mass balances can be found in the Supporting Information.

In order to discuss the influence of the limited adsorption sites more precisely, the loading is converted from mol·kg^{-1} to molecules per unit cell. For this purpose, the loading in mol·kg^{-1} is multiplied by the Avogadro constant N_A and the mass of a unit cell m_{uc}.

$$X\ (\text{molecules/uc}) = X\ (\text{mol/kg})\cdot N_A\ (\text{molecules/mol})\cdot m_{uc}\ (\text{kg/uc}) \quad (6)$$

The mass of a unit cell can be calculated according to eq 7. The masses of the respective atoms A_i are multiplied by the number of atoms N_i and summed up. Subsequently, a conversion is made by the factor $m_u = 1.661 \times 10^{-27}$ kg·u^{-1}.

$$\begin{aligned} m_{uc}\ (\text{kg/uc}) = \Big(&N_{Si}\ (1/\text{uc})\cdot A_{Si}\ (\text{u}) + N_{Al}\ (1/\text{uc})\cdot A_{Al}\ (\text{u}) \\ &+ N_O\ (1/\text{uc})\cdot A_O\ (\text{u}) + N_{Na^+}\ (1/\text{uc})\cdot \\ &A_{Na^+}\ (\text{u}) + N_{Ca^{2+}}\ (1/\text{uc})\cdot A_{Ca^{2+}}\ (\text{u}) \\ &+ N_{H_2O}\ (1/\text{uc})\cdot A_{H_2O}\ (\text{u})\Big)\cdot m_u\ (\text{kg/u}) \end{aligned} \quad (7)$$

The Sips isotherm is used to fit the experimental measurement data. The isotherm parameters X_{mon}, b, and n are fitted individually for each pure component isotherm using nonlinear regression with the Levenberg−Marquardt algorithm by minimizing the error squares.

$$X_{eq}(T, p_{i,eq}) = X_{mon}(T)\cdot\frac{(b(T)\cdot p_{i,eq})^{1/n(T)}}{1 + (b(T)\cdot p_{i,eq})^{1/n(T)}} \quad (8)$$

The selectivity in the binary mixture, which represents the ratio of the alkane and alkene loadings as a function of the respective partial pressures, is used to assess the separation quality.

$$S = \frac{X_{alkene}/X_{alkane}}{p_{alkene}/p_{alkane}} \quad (9)$$

Selectivity alone is not an appropriate measure to assess the separation efficiency for an industrial application, as it does not consider the total load. As a better indicator, we therefore propose a performance factor. This parameter is the product of the selectivity and the loading difference between the alkane and alkene.

$$PF = S\cdot(X_{alkene} - X_{alkane}) \quad (10)$$

4.4. Experimental Uncertainties. Equilibrium loadings determined from experimental data are subject to errors. Since the loadings are calculated from the molar flows, the adsorbent mass, and the concentrations, these variables have an influence on the errors. The concentration determination with μGC has a systematic error of 2% and a statistical error of 0.25%. The systematic error of the MFCs is 1.05%, while the statistical error is 0.2%. The adsorbent mass is determined with a balance that has a systematic error of ±0.02 g and a reproducibility of ±0.01 g. The total error, consisting of systematic and static errors and calculated according to Gaussian error propagation, is between 3.2 and 4% for pure component measurements. For the binary mixture measurements, a calculation of the error leads to very large percentage errors due to the cumulative measurement method and decreasing alkane loadings in the mixture. However, reproducibility measurements show that the experimental error is about 2%. The complete calculation of the experimental errors, as well as a listing of the inaccuracies of the measuring instruments used, can be found in the SI.

■ ASSOCIATED CONTENT

Supporting Information

The Supporting Information is available free of charge at https://pubs.acs.org/doi/10.1021/acsomega.3c09951.

Derivation of the formulas to calculate the pure component and mixture loadings; table of the uncertainties of the apparatuses used and detailed calculation of the statistical error following the Gaussian error propagation; Boltzmann distribution for several differences in heat of adsorption and for different temperatures; pure component and mixture isotherms at −40 and −60 °C for C2 hydrocarbons, −20, −40, and −60 °C for C3 hydrocarbons, and +20, 0, and −20 °C for C4 hydrocarbons; isotherm diagrams with y-axis in mol·kg^{-1}; numerical values of the Sips fitting parameters; and adsorption data of the experiments (PDF)

■ AUTHOR INFORMATION

Corresponding Author

Christoph Pasel − *Thermal Process Engineering, University of Duisburg-Essen, D-47057 Duisburg, Germany*; Email: christoph.pasel@uni-due.de

Authors

Mats Roehnert − *Thermal Process Engineering, University of Duisburg-Essen, D-47057 Duisburg, Germany*; orcid.org/0000-0001-6964-4996

Christian Bläker − *Thermal Process Engineering, University of Duisburg-Essen, D-47057 Duisburg, Germany*; orcid.org/0000-0002-6052-8670

Dieter Bathen − *Thermal Process Engineering, University of Duisburg-Essen, D-47057 Duisburg, Germany; Institute of Energy and Environmental Technology, IUTA e. V., D-47229 Duisburg, Germany*

Complete contact information is available at: https://pubs.acs.org/10.1021/acsomega.3c09951

Author Contributions

The manuscript was written through contributions of all authors. All authors have given approval to the final version of the manuscript.

Notes

The authors declare no competing financial interest.

■ ACKNOWLEDGMENTS

The Chair of Thermal Process Engineering thanks the German Research Foundation (DFG) for financial support within the project BA 2012/15-1. The authors acknowledge support by the Open Access Publication Fund of University of Duisburg-Essen. The adsorbents were kindly provided by Dr. Kristin

Gleichmann, Dr. Jens Zimmermann, and Jakob Eggebrecht from Chemiewerk Bad Köstritz GmbH (CWK).

REFERENCES

(1) Chung, K.; Park, D.; Kim, K.-M.; Lee, C.-H. Adsorption equilibria and kinetics of ethane and ethylene on zeolite 13X pellets. *Microporous Mesoporous Mater.* **2022**, *343*, No. 112199.
(2) Henson, N.; Eckert, J.; Hay, P.; Redondo, A. Adsorption of ethane and ethene in Na−Y studied by inelastic neutron scattering and computation. *Chem. Phys.* **2000**, *261* (1−2), 111−124.
(3) Danner, R. P.; Choi, E. C. F. Mixture Adsorption Equilibria of Ethane and Ethylene on 13X Molecular Sieves. *Ind. Eng. Chem. Fundam.* **1978**, *17* (4), 248−253.
(4) Mofarahi, M.; Salehi, S. M. Pure and binary adsorption isotherms of ethylene and ethane on zeolite 5A. *Adsorption* **2013**, *19* (1), 101−110.
(5) van Miltenburg, A.; Gascon, J.; Zhu, W.; Kapteijn, F.; Moulijn, J. A. Propylene/propane mixture adsorption on faujasite sorbents. *Adsorption* **2008**, *14* (2−3), 309−321.
(6) Jarvelin, H.; Fair, J. R. Adsorptive separation of propylene-propane mixtures. *Ind. Eng. Chem. Res.* **1993**, *32* (10), 2201−2207.
(7) Campo, M. C.; Ribeiro, A. M.; Ferreira, A.; Santos, J. C.; Lutz, C.; Loureiro, J. M.; Rodrigues, A. E. New 13X zeolite for propylene/propane separation by vacuum swing adsorption. *Sep. Purif. Technol.* **2013**, *103*, 60−70.
(8) Huang, Y.-H.; Johnson, J. W.; Liapis, A. I.; Crosser, O. K. Experimental determination of the binary equilibrium adsorption and desorption of propane-propylene mixtures on 13X molecular sieves by a differential sorption bed system and investigation of their equilibrium expressions. *Sep. Technol.* **1994**, *4* (3), 156−166.
(9) Wang, F.; Wang, W.; Huang, S.; Teng, J.; Xie, Z. Experiment and Modeling of Pure and Binary Adsorption of n-Butane and Butene-1 on ZSM-5 Zeolites with Different Si/Al Ratios. *Chin. J. Chem. Eng.* **2007**, *15* (3), 376−386.
(10) Thamm, H.; Stach, H.; Fiebig, W. Calorimetric study of the absorption of n-butane and but-l-ene on a highly dealuminated Y-type zeolite and on silicalite. *Zeolites* **1983**, *3* (2), 95−97.
(11) Ferreira, A. F.; Mittelmeijer-Hazeleger, M. C.; Bliek, A. Adsorption and differential heats of adsorption of normal and isobutane on zeolite MFI. *Microporous Mesoporous Mater.* **2006**, *91* (1−3), 47−52.
(12) Li, K.; Kennedy, E. M.; Chen, S. Z. Adsorption of n-Butane and n-Heptane on 5A Zeolite. *Sep. Sci. Technol.* **1998**, *33* (11), 1571−1584.
(13) Stach, H.; Lohse, U.; Thamm, H.; Schirmer, W. Adsorption equilibria of hydrocarbons on highly dealuminated zeolites. *Zeolites* **1986**, *6* (2), 74−90.
(14) Tielens, F.; Denayer, J. F. M.; Daems, I.; Baron, G. V.; Mortier, W. J.; Geerlings, P. Adsorption of the Butene Isomers in Faujasite: A Combined ab-Initio Theoretical and Experimental Study. *J. Phys. Chem. B* **2003**, *107* (40), 11065−11071.
(15) Birkmann, F.; Pasel, C.; Luckas, M.; Bathen, D. Trace Adsorption of Ethane, Propane, and n -Butane on Microporous Activated Carbon and Zeolite 13X at Low Temperatures. *J. Chem. Eng. Data* **2017**, *62* (7), 1973−1982.
(16) Roehnert, M.; Pasel, C.; Bläker, C.; Bathen, D. Influence of Temperature on the Binary Adsorption of Ethane and Ethene on FAU Zeolites. *J. Chem. Eng. Data* **2023**, *68* (4), 1031−1042.
(17) Bläker, C.; Mauer, V.; Pasel, C.; Dreisbach, F.; Bathen, D. Adsorption mechanisms of ethane, ethene and ethyne on calcium exchanged LTA and FAU zeolites. *Adsorption* **2023**, DOI: 10.1007/s10450-023-00392-0.
(18) Mellot-Draznieks, C.; Buttefey, S.; Boutin, A.; Fuchs, A. H. Placement of cations in NaX faujasite-type zeolite using (N,V,T) Monte Carlo simulations. *Chem. Commun.* **2001**, No. 21, 2200−2201.
(19) Bläker, C.; Pasel, C.; Luckas, M.; Dreisbach, F.; Bathen, D. Investigation of load-dependent heat of adsorption of alkanes and alkenes on zeolites and activated carbon. *Microporous Mesoporous Mater.* **2017**, *241*, 1−10.
(20) Mauer, V.; Bläker, C.; Pasel, C.; Bathen, D. Energetic Characterization of Faujasite Zeolites Using a Sensor Gas Calorimeter. *Catalysts* **2021**, *11* (1), No. 98.
(21) Kulprathipanja, S. *Zeolites in Industrial Separation and Catalysis*; Wiley-VCH Verlag GmbH & Co. KGaA, 2010.
(22) Yang, R. T. *Adsorbents: Fundamentals and Applications*; John Wiley & Sons, Inc, 2003.
(23) Jaramillo, E.; Auerbach, S. M. New Force Field for Na Cations in Faujasite-Type Zeolites. *J. Phys. Chem. B* **1999**, *103* (44), 9589−9594.
(24) Frising, T.; Leflaive, P. Extraframework cation distributions in X and Y faujasite zeolites: A review. *Microporous Mesoporous Mater.* **2008**, *114* (1−3), 27−63.
(25) Buttefey, S.; Boutin, A.; Mellot-Draznieks, C.; Fuchs, A. H. A Simple Model for Predicting the Na + Distribution in Anhydrous NaY and NaX Zeolites. *J. Phys. Chem. B* **2001**, *105* (39), 9569−9575.
(26) Allinger, N. L. Conformational analysis. 130. MM2. A hydrocarbon force field utilizing V1 and V2 torsional terms. *J. Am. Chem. Soc.* **1977**, *99* (25), 8127−8134.
(27) Reid, C. R.; Thomas, K. M. Adsorption Kinetics and Size Exclusion Properties of Probe Molecules for the Selective Porosity in a Carbon Molecular Sieve Used for Air Separation. *J. Phys. Chem. B* **2001**, *105* (43), 10619−10629.
(28) Webster, C. E.; Drago, R. S.; Zerner, M. C. Molecular Dimensions for Adsorptives. *J. Am. Chem. Soc.* **1998**, *120* (22), 5509−5516.
(29) National library of Medicine. PubChem. https://pubchem.ncbi.nlm.nih.gov/. (accessed March 02, 2024).
(30) Buckingham, A. D.; Disch, R. L.; Dunmur, D. A. Quadrupole moments of some simple molecules. *J. Am. Chem. Soc.* **1968**, *90* (12), 3104−3107.
(31) Buckingham, A. D.; Graham, C.; Williams, J. H. Electric field-gradient-induced birefringence in N 2, C 2 H 6, C 3 H 6, Cl 2, N 2 O and CH 3 F. *Mol. Phys.* **1983**, *49* (3), 703−710.
(32) Lide, D. R. *CRC Handbook of Chemistry and Physics: A Ready-Reference Book of Chemical and Physical Data*, 96th ed.; CRC Press, 2015.
(33) Kast, W. *Adsorption aus der Gasphase:Ingenieurwissenschaftliche Grundlagen und Technische Verfahren*; Wiley-VCH, 1988.
(34) Auerbach, S. M.; Carrado, K. A.; Dutta, P. K. *Handbook of Zeolite Science and Technology*; CRC Press, 2003.
(35) Schmittmann, S.; Pasel, C.; Luckas, M.; Bathen, D. Trace Adsorption of Light Hydrocarbons at Low Temperatures: Influence of Carrier Gas Coadsorption. *Ind. Eng. Chem. Res.* **2019**, *58* (24), 10540−10549.
(36) Bey, O.; Eigenberger, G. Fluid flow through catalyst filled tubes. *Chem. Eng. Sci.* **1997**, *52* (8), 1365−1376.

https://doi.org/10.1021/acsomega.3c09951
ACS Omega 2024, 9, 37548−37559

DOI: 10.1021/acsomega.3c09951
URN: urn:nbn:de:hbz:465-20241220-124632-9